Metabolic role of fatty acid binding protein 7 in mediating triple-negative breast cancer cell death via PPAR-α signaling[S]

Soke Chee Kwong,* Amira Hajirah Abd Jamil,† Anthony Rhodes,§, Nur Aishah Taib,††,§§ and Ivy Chung[1],*,§§**

Departments of Pharmacology,* Pharmacy,† Pathology,** and Surgery†† and University of Malaya Cancer Research Institute,§§ Faculty of Medicine, University of Malaya, 50603 Kuala Lumpur, Malaysia; and School of Medicine, Faculty of Health and Medical Sciences,§ Taylor's University, Lakeside Campus, 47500 Subang Jaya, Selangor, Malaysia

Abstract Triple-negative breast cancer (TNBC) is the most aggressive subtype of breast cancer, partly due to the lack of targeted therapy available. Cancer cells heavily reprogram their metabolism and acquire metabolic plasticity to satisfy the high-energy demand due to uncontrolled proliferation. Accumulating evidence shows that deregulated lipid metabolism affects cancer cell survival, and therefore we sought to understand the function of fatty acid binding protein 7 (FABP7), which is expressed predominantly in TNBC tissues. As FABP7 was not detected in the TNBC cell lines tested, Hs578T and MDA-MB-231 cells were transduced with lentiviral particles containing either FABP7 open reading frame or red fluorescent protein. During serum starvation, when lipids were significantly reduced, FABP7 decreased the viability of Hs578T, but not of MDA-MB-231, cells. FABP7-overexpressing Hs578T (Hs-FABP7) cells failed to efficiently utilize other available bioenergetic substrates such as glucose to sustain ATP production, which led to S/G2 phase arrest and cell death. We further showed that this metabolic phenotype was mediated by PPAR-α signaling, despite the lack of fatty acids in culture media, as Hs-FABP7 cells attempted to survive. This study provides imperative evidence of metabolic vulnerabilities driven by FABP7 via PPAR-α signaling.— Kwong, S. C., A. H. A. Jamil, A. Rhodes, N. A. Taib, and I. Chung. **Metabolic role of fatty acid binding protein 7 in mediating triple-negative breast cancer cell death via PPAR-α signaling. *J. Lipid Res*. 2019.** 60: **1807–1817.**

Supplementary key words fatty acid binding protein • peroxisome proliferator-activated receptor alpha • cancer • nutrient deprivation • fatty acid metabolism • metabolic adaptation

Triple-negative breast cancer (TNBC) is a subtype of breast cancer that lacks the expression of estrogen receptors (ERs) and progesterone receptors (PRs), as well as human epidermal growth factor receptor 2 (HER2). It is the most aggressive subtype of breast cancer, affecting about 15–20% of total breast cancer cases. Compared with other subtypes, TNBC tumors are associated with higher histologic grade and larger tumor size (1, 2). The current standard regimen for TNBC patients is a combination of surgery and chemotherapy (3), which often fails to effectively slow down the tumor progression. Hence, TNBC patients have lower overall survival (81% vs. 91%) and disease-free survival (72% vs. 86%) compared with non-TNBC patients (4). Given the lack of ER and HER2 in this subtype, there is no molecular characterization that allows this subtype to be targeted.

Uncontrolled proliferation of cancer cells is metabolically demanding. The metabolic pathways utilized by cancer cells to sustain high-energy demands and biosynthesis differ from those employed by healthy cells (5). Challenged by hostile environments such as hypoxia and acute interruptions in nutrient availability, cancer cells typically develop metabolic plasticity, which enables the utilization of available nutrients as bioenergetic substrates. This metabolic flexibility allows maintained ATP production under varying physiological and pathological conditions and is primarily regulated by substrate concentration, hormone levels, blood flow, oxygen supply, and workload (6).

Cancer-associated changes in cellular metabolism may also be a direct consequence of oncogenic signal transduction.

This work was supported by University of Malaya High Impact Research Grant UM.C/HIR/MOHE/06; University of Malaya Research Grant RP019-b; and the Translational Core Laboratory, Faculty of Medicine, University of Malaya. The authors declare no conflicts of interest.

Manuscript received 7 January 2019 and in revised form 6 August 2019.

Published, JLR Papers in Press, September 4, 2019
DOI https://doi.org/10.1194/jlr.M092379

Abbreviations: CPT1A, carnitine palmitoyltransferase 1A; ER, estrogen receptor; FABP, fatty acid binding protein; FAO, FA oxidation; GEO, Gene Expression Omnibus; GLS1, glutaminase 1; GLUT1, glucose transporter 1; HER2, human epidermal growth factor receptor 2; MCAD, medium-chain acyl-CoA dehydrogenase; MTT, methyl thiazolyl tetrazolium; OCR, oxygen consumption rate; OD, optical density; PR, progesterone receptor; TNBC, triple-negative breast cancer.

[1]To whom correspondence should be addressed.
e-mail: ivychung@ummc.edu.my

[S] The online version of this article (available at http://www.jlr.org) contains a supplement.

AKT activation augments the Warburg effect and renders the cancer cells addicted to glucose (7). Myc protein promotes mitochondrial glutaminolysis and glutamine addiction by shunting glucose away from mitochondrial metabolism (8). Cancer cells that fail to demonstrate metabolic flexibility during nutrient deprivation could become vulnerable in their survival (9). Hence, metabolic vulnerabilities exhibited by cancer cells can be targeted for cancer management (6, 10).

Alterations in lipid- and cholesterol-associated pathways encountered in tumors are now increasingly recognized and more frequently described (11, 12), but not completely understood. Many cancer types show a strong lipid avidity, in which increasing uptake of exogenous lipid sources (13) or overactivation of endogenous lipid synthesis (14) is observed. Fatty acid binding protein 7 (FABP7), a member of the FABP intracellular lipid chaperone family, has been shown to be upregulated in TNBC compared with other breast cancer subtypes (15, 16). FABPs regulates lipid metabolism by increasing fatty acid uptake (17), fatty acid oxidation (FAO) (18), and lipolysis (19). Yet, in TNBC, correlation of FABP7 expression and disease prognosis is debatable. While one study showed that FABP7 expression correlates with lower overall and recurrence-free survival (20), several have shown that FABP7-positive basal tumors (synonymous with TNBC) are associated with better prognosis (21, 22). It is unclear, at this point, how FABP7-governed pathways impact the survival of TNBC.

In this study, we explored the roles of FABP7 in adaptation to nutrient depletion in TNBC cell lines. We showed that overexpression of FABP7 decreased the viability of Hs578T cells during serum starvation. This led to cell-cycle arrest and a significant increase in cell death. We further showed that this phenotype was mediated by PPAR-α-regulated genes.

MATERIALS AND METHODS

Cell culture

All cell lines used in this study were purchased from American Type Culture Collection (Gaithersburg, MD). They were cultured in medium according to the manufacturer's protocol and supplemented with 10% FBS and 1% penicillin/streptomycin (Life Technologies, Grand Island, NY), unless specified otherwise. Hs578T, MCF7, MDA-MB-231, and MDA-MB-435S were maintained in DMEM high glucose while BT474 was cultured in MEM. The cell lines were incubated at 37°C and 5% CO_2 atmosphere.

For nutrient-deprivation experiments, the cells were first seeded in complete medium (10% FBS). The next day (hereafter referred to as 0 h), the cells were washed once with PBS and replaced with nutrient-deprived medium. For the glucose- and glutamine-starvation experiments, 10% FBS were added into the basal medium. Basal medium used for glucose starvation was glucose-free DMEM (Life Technologies, catalog no. 11966-025) that contained 4 mM L-glutamine. For the glutamine-starvation experiment, glutamine-free DMEM (Life Technologies, catalog no. 11960-044) containing 25 mM glucose was used. The serum-starvation experiment mimicked a culture condition with deprived lipids. The cells were challenged with serum-free DMEM (Life Technologies, catalog no. 11965-092) that contains high glucose (25 mM) with L-glutamine (4 mM), but without sodium pyruvate, HEPES, lipids, and growth factors.

The PPAR-α antagonist (GW6471) was obtained from Santa Cruz Biotechnology (Santa Cruz, CA) and used at a nonlethal concentration (2 μM).

Data mining at GEO database

A microarray profile of selected TNBC was obtained from the publicly available Gene Expression Omnibus (GEO) database. The search keyword used was "triple negative breast cancer," and the results were filtered with "*Homo sapiens*." The search was conducted from September 1 to 30, 2018.

Generation of FABP7-transduced TNBC cell lines

TNBC cell lines Hs578T and MDA-MB-231 were transduced with FABP7 gene using Thermo Scientific Precision LentiORF constructs at MOI 10 (Clone ID: PLOHS_100004067). For their control counterparts, the cells were transduced with Precision LentiORF RFP (catalog no. OHS5833). The transduced cells were selected with blasticidin for 30 days to generate stable cell line.

MTT assay

Cells were seeded in 96-well plates and subjected to different growth conditions. At time of termination, 10 μl of methyl thiazolyl tetrazolium (MTT) solution (5 mg/ml) (Sigma, St. Louis, MO) was added into each well for 4 h, before the addition of 100 μl of 10% sodium dodecyl sulfate (SDS) to dissolve the formazan crystals overnight. Absorbance was measured at 575 nm with reference to 650 nm. All experiments were performed in triplicate and repeated three times.

RNA extraction and qRT-PCR

Total RNA extraction was carried out using Trizol (Invitrogen, Carlsbad, CA) following the recommended protocol. About 500 ng of RNA was converted into cDNA using DyNAmo cDNA synthesis kit (Finnzymes, Vantaa, Finland). For quantitative RT-PCR (qRT-PCR), 5 ng/μl cDNA template was added into pool solution containing 5× HOT FIREPol EvaGreen qPCR Mix (Solis Biodyne, Tartu, Estonia), 10 pmol/μl forward and reverse primers, and UltraPure distilled water. ABI StepOne Plus (Applied Biosystem, Foster City, CA) was used, and 40 cycles of amplification were performed. The expression of metabolic genes was normalized to housekeeping genes 18S rRNA and ribosomal protein L13a. Sequence of the primers used is described in supplemental Table S1.

Protein extraction and Western blotting

Protein lysate was harvested by scraping the cells in cold PBS. After centrifugation, PBS was discarded, and the cells were incubated in lysis buffer (0.1% Triton X-100, 0.1% SDS, 50 mM Tris, 150 mM NaCl, 1× phosphatase, and 1× protease inhibitors) for 30 min on ice. The mixture was centrifuged for 20 min, and supernatant was collected as protein lysate. Protein concentration was quantified using Bradford assay (Bio-Rad, Hercules, CA). A total of 30 μg of protein was resolved on 15% SDS-PAGE prior to transferring on PVDF membrane. Target proteins were detected using primary Abs FABP7 (Cell Signaling Technology) and ECL prime Western blotting detection reagent (Amersham, GE Healthcare Lifesciences, Sweden) before being visualized with gel-documentation system (Biospectrum 410, UVP).

BrdU cell-proliferation assay

The BrdU cell-proliferation assay kit (Cell Signaling Technology, Beverly, MA) was used to measure the cell-proliferation rate at 24, 48, and 72 h after serum starvation. The data were normalized to their counterparts cultured in complete medium. The

cells were incubated with 10X BrdU solution for three h, prior to fixation for 30 min and staining with 1× BrdU Detection Antibody for 1 h. The stained cells were washed and incubated with 1× HRP-conjugated secondary antibody solution for 30 min, before TMB solution was added. STOP solution was added after 15 min, and absorbance was read at 450 nm.

Cell-cycle analysis with propidium iodide

Cell-cycle analysis was conducted on the cells at 0, 24, 48, and 72 h after serum starvation. The cells were fixed with 70% ethanol at 4°C for 30 min, before two washes with PBS. Enzymatic removal of RNA was achieved by incubating the cells with 100 μg/ml RNase for 15 min before DNA staining with 50 μg/ml propidium iodide. The cells were analyzed using a BD FACSCanto II flow cytometer, and the cell-cycle distribution of the cell was analyzed with Modfit LT software. The samples were run in triplicates, and the mean value was calculated.

Annexin V apoptosis assay

Cells were harvested for apoptosis assay at 0, 24, 48, and 72 h after serum starvation. Floating cells in the culture medium and the trypsinized cells were collected and washed once with ice-cold PBS, before they were resuspended in 100 μl of assay buffer (1 part buffer: 9 parts distilled water) with 5 μl of annexin V-PE and 5 μl of 7AAD (BD Bioscience, Franklin Lakes, NJ). The cells were vortexed gently and kept in the dark for 15 min, before adding 400 μl of buffer. The staining was analyzed using a BD FACSCanto II flow cytometer and viewed using FACS DiVa Software (BD Bioscience, San Jose, CA). All samples were run in triplicates, and mean value was calculated.

Metabolic activity assays

GAPDH, glutaminase (GSL), and FAO enzyme activities were measured using calorimetric assay kits from Biomedical Research Service Center, State University of New York (Buffalo, NY). All samples were harvested using 1× Cell Lysis Solution. Protein concentration of the samples was assessed with a Bradford assay and normalized to 1 mg/ml. GAPDH activity was measured using GAPDH enzyme assay kit (catalog no. E-101). Briefly, 10 μl of sample or water (as blank) was incubated in 50 μl of GAPDH assay solution. After gentle agitation, the plate was kept in a non-CO_2 incubator at 37°C for 60 min. For GSL assay (catalog no. E-133), 10 μl of sample was incubated in either 40 μl of glutamine solution or water. Following a 2 h incubation period in a non-CO_2 incubator at 37°C, 50 μl of TA assay solution was added, and the plate was further incubated for another 1 h. For FAO enzyme assay (catalog no. E-141), 50 μl of FAO Assay Solution or control solution was added to 10 μl of the protein sample. The plate was kept in a non-CO_2 incubator at 37°C for 60 min. All experiments were terminated by adding 50 μl of 3% acetic acid, and the plate was read at optical density of 492 nm (OD 492) with a spectrophotometer. Blank reading was subtracted from the sample reading. GAPDH activity in IU/l unit was determined by multiplying OD by 16.98. Glutaminase (GLS) activity in IU/l unit = μmol/(l·min) = (OD × 1,000 × 150 μl) ÷ (120 min × 0.6 cm × 18 × 10 μl) = OD × 11.58. For FAO assay, the subtracted OD represents the FAO activity of the sample.

Measurement of OCR

Basal oxygen consumption rate (OCR) was carried out with a Mito Fuel Flex Test Kit on XFe96 Bioanalyzer (Agilent). Briefly, 4,000 cells were seeded on a Seahorse XF96-well assay plate in complete medium. The cells grown in complete medium were terminated at 24 h after seeding. For the serum-starvation experiment, the cells were left incubated overnight before they were washed with PBS and incubated in serum-free medium for 24 h. Upon termination, all wells were replaced with assay medium, and baseline OCR was immediately measured for 18 min. The basal OCR was normalized to protein concentration of the cells.

Immunofluorescence staining

The cells were seeded on a coverslip in complete medium. After overnight incubation, the cells were either harvested or challenged with serum-free medium for 24 h. The cells were fixed with 4% formaldehyde for 30 min, washed with PBS, and permeabilized in 0.1% Triton X-100 for 1 h. The cells were incubated with FABP7 primary antibody (1:2,000; Cell Signaling catalog no. 13347S) and PPAR-α primary antibody (1:400; Santa Cruz Biotechnology, catalog no. sc-398394), followed by Alexa Fluor 488 donkey anti-rabbit IgG and Alexa Fluor 647 goat anti-mouse IgG (Invitrogen, Thermofisher Scientific). The incubation time was 90 min for primary antibody and 60 min for secondary antibody. The cells were washed three times with PBS after staining with each antibody. All the procedures were carried out on ice. The coverslips were mounted with 4′,6-diamidino-2-phenylindole (DAPI) mounting medium (Vector Laboratories Cat#H-1200) and analyzed with a Leica TCS SP5 II laser microscope (Leica, Heidelberg, Germany) using 60× objective.

Statistical analysis

Statistical analysis assessing the difference between the means of two groups was performed using Student's *t*-test with GraphPad-Prism (GraphPad Software, San Diego, CA). A *P*-value <0.05 was considered statistically significant.

RESULTS

FABP7 overexpression decreased viability of Hs578T, but not MDA-MB-231, cells in serum starvation

The expression of FABP7 was determined in human breast cancer tissues and TNBC cell lines. Analysis from the GEO database (dataset GSE65194) revealed that FABP7 expression was significantly higher in TNBC (n = 55) compared with non-TNBC (n = 98) subtypes (**Fig. 1A**). When examined in a panel of breast cancer cell lines, FABP7 showed low expression in all cells including MCF7 (luminal A), BT474 (luminal B), MDA-MB-231, and Hs578T (TNBC) cells, when compared with MDA-MB-435S, a melanoma cell line reported to express high FABP7 (Fig. 1B). Correspondingly, FABP7 protein was not detected in these breast cancer cell lines (Fig. 1C).

To understand the functional role of FABP7 in TNBC cells, we established FABP7-overexpressing Hs578T and MDA-MB-231 TNBC cells by transduction using lentiviral particles containing FABP7 open reading frame (Hs-FABP7 and 231-FABP7, respectively) and their control counterparts using lentiviral particles containing red fluorescent protein (Hs-RFP and 231-RFP, respectively) (Fig. 1D). When the cells were cultured in complete medium for 72 h, there was no difference in cell growth between cells expressing FABP7 and their respective RFP controls (**Fig. 2**). However, when cultured in glucose- or glutamine-deprived condition, both FABP7-overexpressing cells and RFP controls demonstrated substantial reduction in cell viability with greater effect observed in glucose-deprived than glutamine-deprived medium (Fig. 2A,B).

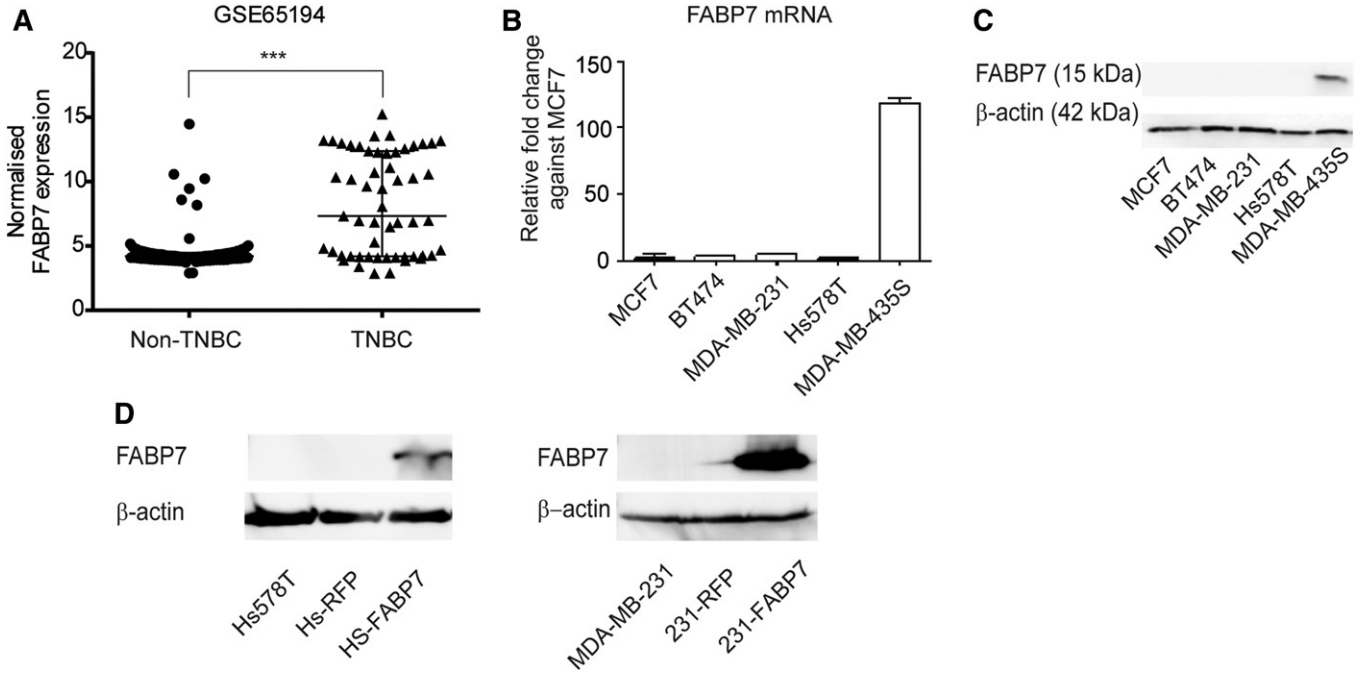

Fig. 1. Generation of FABP7-overexpressing TNBC cells. A: The result shows data mining on FABP7 expression in non-TNBC versus TNBC tumors from online database Geodataset. *** $P < 0.0001$. FABP7 mRNA (B) and protein expressions (C) of breast cancer cell lines were analyzed using qRT-PCR and Western blotting, respectively. D: Western blot was performed for FABP7 protein detection to confirm FABP7 expression posttransduction in the selected TNBC cell lines. Data represent the mean ± SEM of duplicates and are representative of two independent experiments.

Interestingly, when lipids were significantly reduced during serum starvation, overexpression of FABP7 resulted in decreased viability of Hs578T cells (Fig. 2C). At 24 h after serum starvation, the cell viability of Hs-FABP7 cells decreased by 10%, which progressively decreased to approximately 70% at 72 h after starvation ($P < 0.0001$ vs. Hs-RFP cells). Cell viability of Hs-RFP cells was not affected by serum starvation, indicating that the decreased viability in Hs-FABP7 cells may be related to FABP7 expression. This phenotype appeared to be specific to Hs578T cells, as FABP7 expression did not affect the viability of MDA-MB-231 cells in serum-free medium (Fig. 2C).

Decreased viability of Hs-FABP7 cells in serum starvation was due to reduced proliferation, cell-cycle arrest, and cell death

The reduction in cell viability of Hs-FABP7 cells during serum starvation resulted from a decrease in cell proliferation. Hs-FABP7 cells demonstrated a 70% reduction in BrdU uptake as early as 24 h after serum starvation, whereas the control Hs-RFP cells only showed a decrease by 20% (**Fig. 3A**). The nonresponsive MDA-MB-231 cells maintained their proliferation rate in the range of 85–89% during serum starvation, regardless of FABP7 expression.

Flow-cytometry analysis showed that FABP7 induced cell-cycle arrest in Hs578T cells during serum starvation (Fig. 3B and supplemental Fig. S1). Hs-RFP cells showed a higher distribution of cells (∼80%) in G1 phase throughout serum starvation, indicating that the cells were able to complete the cell cycle and proliferate, parallel to increased cell viability over time. In contrast, Hs-FABP7 cells demonstrated a consistently higher percentage of cells in S and G2 phase upon serum starvation. For instance, at 48 h after serum starvation, 24% of Hs-FABP7 cells were accumulated in S phase and 8.23% in G2 phase, whereas only 5.15% and 1.99% of Hs-RFP cells were detected at S and G2 phase ($P = 0.0052$ for S phase and $P = 0.0241$ for G2 phase). The percentage of cells in S/G2 phase increased to 40.15% in Hs-FABP7 cells compared with 14.29% in Hs-RFP cells at 72 h after serum starvation. Cell arrest in S/G2 phase in Hs-FABP7 cells may partly contribute to the decreased cell viability during serum starvation. This effect was not observed in MDA-MB-231 cells (Fig. 3B).

The decrease in Hs-FABP7 cell viability during serum starvation was potentially attributed to apoptosis and necrosis (Fig. 3C). More necrotic cell death and late apoptosis was observed in Hs-FABP7 cells (34.26% and 21.3%) than in Hs-RFP cells (18.83% and 4.63%) at 72 h after serum starvation ($P < 0.0001$). Upon serum starvation, increasing cell death was observed in MDA-MB-231 cells, but with no significant difference observed between 231-RFP and 231-FABP7 cells. Taken together, the decreased cell viability in Hs-FABP7 cells during serum starvation was due to reduced proliferation rate, cell cycle arrest at S and G2 phase, and cell death.

Perturbations in the metabolism and mitochondrial oxygen consumption in Hs-FABP7 cells during serum starvation

Given the role of FABP7 in fatty acid metabolism, we investigated the mechanism of FABP7-induced cell death by exploring a panel of genes and enzyme activities involved in the metabolism of glucose, glutamine, and fatty acid (**Fig. 4** and supplemental Figs. S2, S3).

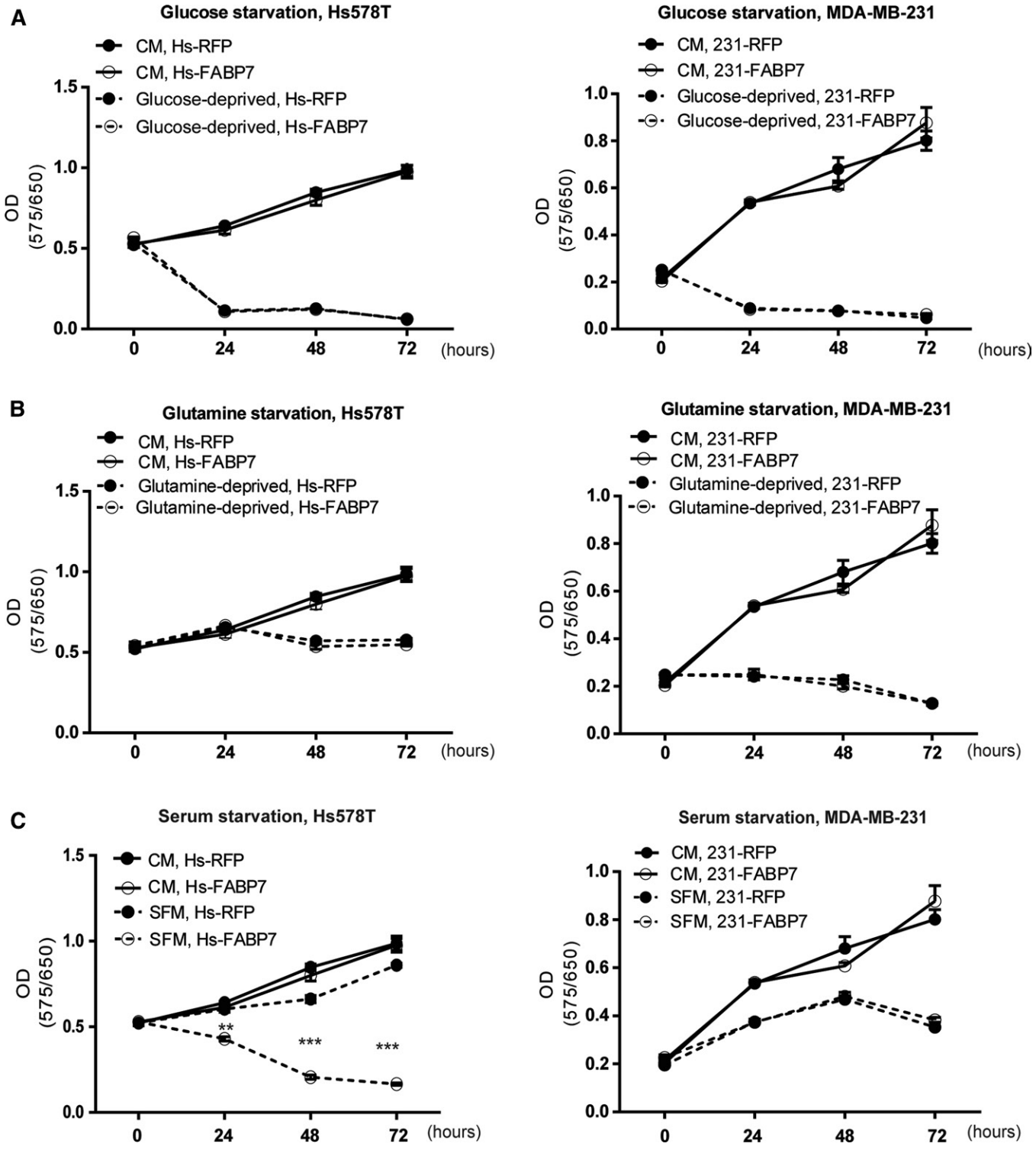

Fig. 2. The effect of FABP7 on TNBC cell viability in various nutrient-deprived conditions. MTT assay was used to investigate the viability of Hs578T and MDA-MB-231 cells in glucose-starved (A), glutamine-starved (B), and serum-starved (C) conditions. The cells were cultured in either complete medium or nutrient-deprived medium. Data represent the mean ± SEM of triplicates and are representative of three independent experiments. ** $P < 0.001$; *** $P < 0.0001$. CM, complete medium; SFM, serum-free medium.

In complete medium, despite the increase in glucose transporter 1 (GLUT1) mRNA expression, glycolysis-related genes phosphofructokinase 1 (PFK1) and GAPDH remained unchanged in Hs-FABP7 cells, whereas the genes regulating FAO, carnitine palmitoyltransferase 1A (CPT1A), and medium-chain acyl-CoA dehydrogenase (MCAD) were markedly upregulated (Fig. 4A). In Hs-FABP7 cells, the expression of GLS1, encoding the rate-limiting enzyme for glutaminolysis, was not significantly different than in Hs-RFP cells. When cultured in complete medium, Hs-FABP7 cells did not show any differences in GAPDH, GLS, and FAO activities when compared with Hs-RFP cells

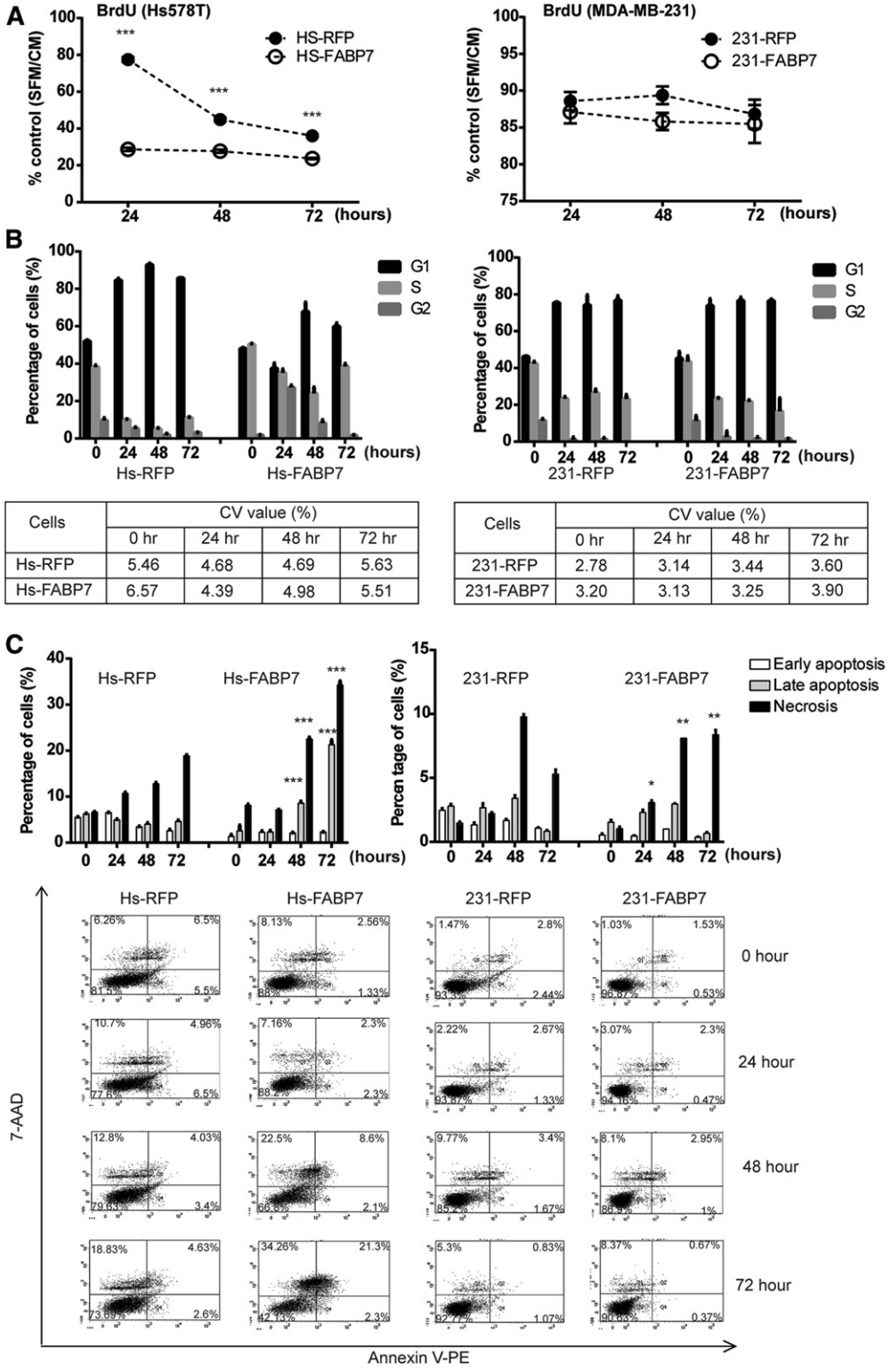

Cells	CV value (%)			
	0 hr	24 hr	48 hr	72 hr
Hs-RFP	5.46	4.68	4.69	5.63
Hs-FABP7	6.57	4.39	4.98	5.51

Cells	CV value (%)			
	0 hr	24 hr	48 hr	72 hr
231-RFP	2.78	3.14	3.44	3.60
231-FABP7	3.20	3.13	3.25	3.90

Fig. 3. Decreased viability of Hs-FABP7 cells in serum starvation was due to decreased proliferation, cell-cycle arrest, and cell death. A: Proliferation of Hs578T and MDA-MB-231 cells cultured in serum-starved conditions and in complete medium for 24, 48, and 72 h was measured using BrdU assay. Data shown are the mean ± SEM of triplicates and are representative of two independent experiments. B: Effects of FABP7 on cell cycle in serum starvation were detected by flow cytometry using propidium iodide staining. The analysis on cell-cycle distribution were performed using Modfit LT software. Data shown are the mean ± SEM of triplicates and are representative of three independent experiments; coefficient of variation (CV) values shown were also the average of the triplicates. C: Percentage of necrotic and apoptotic cells was measured using an annexin V/7-AAD apoptosis assay. Data shown are the mean ± SEM of triplicates and are representative of two independent experiments. The *P* value represents the statistical significance when the Hs-FABP7 group was compared with the control group. * $P < 0.05$; ** $P < 0.001$; *** $P < 0.0001$.

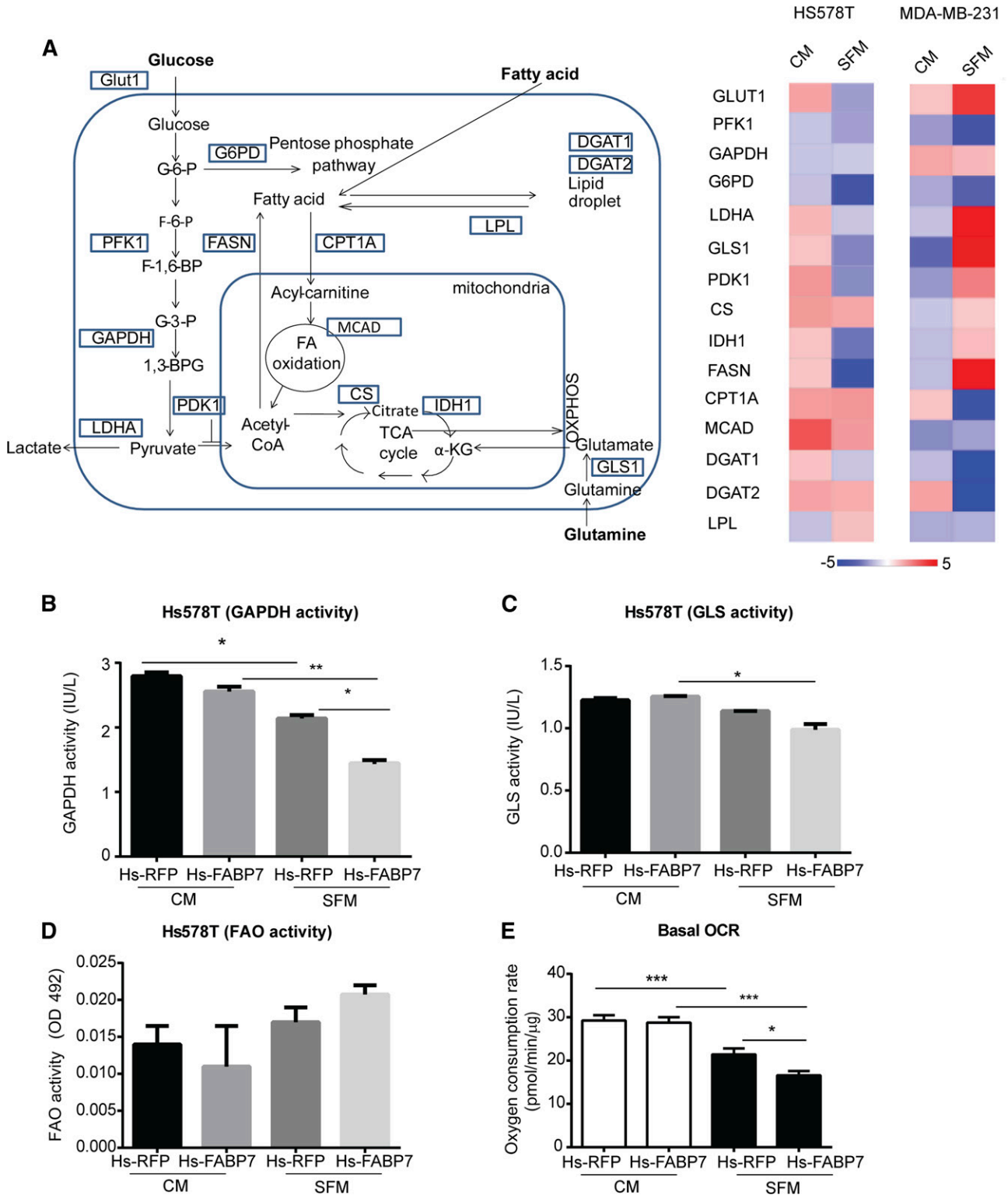

Fig. 4. FABP7 altered the metabolism in Hs578T cells during serum starvation. A: Diagram showing genes involved in glycolysis, glutaminolysis, and FA metabolism, as highlighted in the box. The heatmap compares the expression of metabolic genes in FABP7-overexpressing cells to control cells cultured in complete medium and serum-free medium. The genes were normalized to housekeeping gene 18S rRNA. Data represent the mean ± SEM of duplicates and are representative of two independent experiments. Enzymatic assays evaluating GAPDH (B), GLS (C), and FAO (D) activities were conducted. Data shown are mean ± SEM of duplicates. E: Basal OCR of the cells (n = 18 for each group) was measured with a Seahorse Mito Fuel Flex Test Kit. Data shown are mean ± SEM of replicates, a representative of two experiments. * $P < 0.05$; ** $P < 0.01$; *** $P < 0.0001$. CM, complete medium; SFM, serum-free medium.

(Fig. 4B–D). Subsequently, mitochondrial OCR was similar in Hs-FABP7 cells and in the control Hs-RFP cells (Fig. 4E).

However, when challenged with serum starvation, a widespread downregulation of glucose and glutamine metabolism-related genes were observed in Hs-FABP7 cells when compared with Hs-RFP cells. Interestingly, despite the absence of serum (lipids) during serum starvation, the gene expression of CPT1A and MCAD was about 2-fold higher in Hs-FABP7 cells than Hs-RFP cells (Fig. 4A). Serum starvation generally decreased glycolytic enzyme activity in Hs578T cells, but FABP7-overexpressing cells had a further 30% reduction ($P = 0.0121$) in GAPDH activity compared with Hs-RFP cells (Fig. 4B). Although GLS activity remained not significantly different in both cells during serum starvation, GLS activity was significantly lower ($P = 0.0296$) in Hs-FABP7 cells cultured in serum starvation than in complete medium (Fig. 4C). Interestingly, FAO activity in Hs-FABP7 remained similar with the control Hs-RFP cells (Fig. 4D), despite upregulation of FAO-related genes. This may be explained by the lack of fatty acid in the culture medium to activate the metabolic pathway. Consequently, mitochondrial oxidative capacity of both Hs-RFP and Hs-FABP7 cells was generally lower during serum starvation ($P = 0.0001$ for both cells); however, Hs-FABP7 cells had much lower OCR (16.69 pmol/min/μg) compared with Hs-RFP cells (21.7 pmol/min/μg) ($P < 0.05$) (Fig. 4E). These data indicate a lower mitochondrial oxidative capacity particularly in Hs-FABP7 cells, probably due to limited bioenergetic substrates during serum starvation.

It is worthwhile to note that, unlike Hs578T, MDA-MB-231 cells showed a rather different metabolic profile, as indicated by the expression of metabolic genes (Fig. 4A and supplemental Fig. S2B). When cultured in complete medium, although FABP7 was not affecting the cell viability, glycolysis was upregulated in 231-FABP7 cells, with about a 1.7-fold increase in GAPDH expression. Meanwhile, a 4-fold decrease in GLS1 expression was observed, indicative of a downregulation of the glutaminolysis pathway. Upon serum starvation, 231-FABP7 cells demonstrated a marked increase in glucose and glutamine metabolism-related genes, with more than 4-fold increase in GLUT1 and GLS1 expression.

Taken together, our data show that Hs-FABP7 cells, when challenged with a serum-starved condition, were not able to metabolically adapt and effectively utilize other available energetic substrates, especially glucose, and, as a consequence, could not survive.

PPAR-α signaling mediated FABP7-induced cell death in Hs578T cells under serum starvation

The upregulation of CPT1A and MCAD mRNA, accompanied with a downregulation of Glut1 mRNA in Hs-FABP7 cells, indicated a possible role of PPAR-α signaling, as these genes are direct targets of PPAR-α transcription factor. Immunofluorescence staining showed that the expression of PPAR-α protein was increased in the nucleus during serum starvation (**Fig. 5A** and supplemental Fig. S4A). Similarly, FABP7 protein was observed to translocate into the nucleus (Fig. 5A and supplemental Fig. S4B) in Hs-FABP7 cells upon serum starvation, potentially acting as fatty acid chaperones to deliver ligands to PPAR-α protein (23). This suggests that nuclear localization of FABP7 enhanced the action of PPAR-α transcriptional activity during serum starvation in Hs-FABP7 cells.

To investigate whether PPAR-α activation was responsible for FABP7-mediated inhibition of cell viability in Hs-FABP7 cells, we treated the cells with a PPAR-α-specific inhibitor (GW6471). In both Hs578T and MDA-MB-231 cells, treatment of GW6471 at a concentration of 2 μM in complete medium had no significant effect on cell viability (Fig. 5B). Yet, the same concentration of GW6471 reversed the cell-growth inhibition observed in Hs-FABP7 cells when exposed to serum-starved conditions (Fig. 5B and supplemental Fig. S5). Subsequent gene-expression analysis revealed that PPAR-α target genes were downregulated (CPT1A: −2.43-fold; MCAD: −1.54-fold), when compared with vehicle-treated cells (Fig. 5C). A significant ∼2-fold increase of GLUT1, PFK1, glucose-6-phosphate dehydrogenase (G6PD), and isocitrate dehydrogenase 1 (IDH1) mRNA expression was observed in GW6471-treated Hs-FABP7 cells (Fig. 5C), indicating that the rescue of cell viability may be due to the switch from lipid to glucose as bioenergetic substrates in these cells. Taken together, FABP7-induced cell death in Hs578T cells during serum starvation is due to activated PPAR-α signaling.

DISCUSSION

In this study, we showed that overexpression of FABP7 disabled TNBC cell line Hs578T to metabolically adapt during serum starvation. FABP7-overexpressing cells failed to efficiently utilize glucose as bioenergetics substrates, when challenged with serum starvation. This was accompanied by increased expression of genes controlling FAO as it attempts to utilize free fatty acids liberated by lipolysis from the lipid storage that resulted from preexposure to complete medium (24). However, as free fatty acid storage was depleted, serum-starved FABP7-overexpressing cells were not able to further metabolically adapt and sustain ATP production. The failure of the cells to efficiently utilize glucose for ATP generation leads to cell death. We further showed that the metabolic impact of FABP7 in Hs578T cells during serum starvation is mediated by PPAR-α signaling.

FABP7 is predominantly expressed in the nervous system and mammary gland. In the mammary gland, FABP7 inhibits proliferation and promotes differentiation of mammary cells (25). Similarly, in the nervous system, FABP7 is involved in the differentiation of neurons and development of the cortex (26, 27). The expression of FABP7 at the edge of astrocytes also suggested that FABP7 may regulate the motility of astrocytes by increasing the uptake of polyunsaturated fatty acids (28). Yet, the evidence of FABP7 expression in TNBC cell lines was rather limited (20, 29). A previous study demonstrating the function of endogenous FABP7 in TNBC was reported using MDA-MB-435S, a melanoma cell line formerly misidentified as a TNBC cell line (30). Our study, however, provides evidence on the

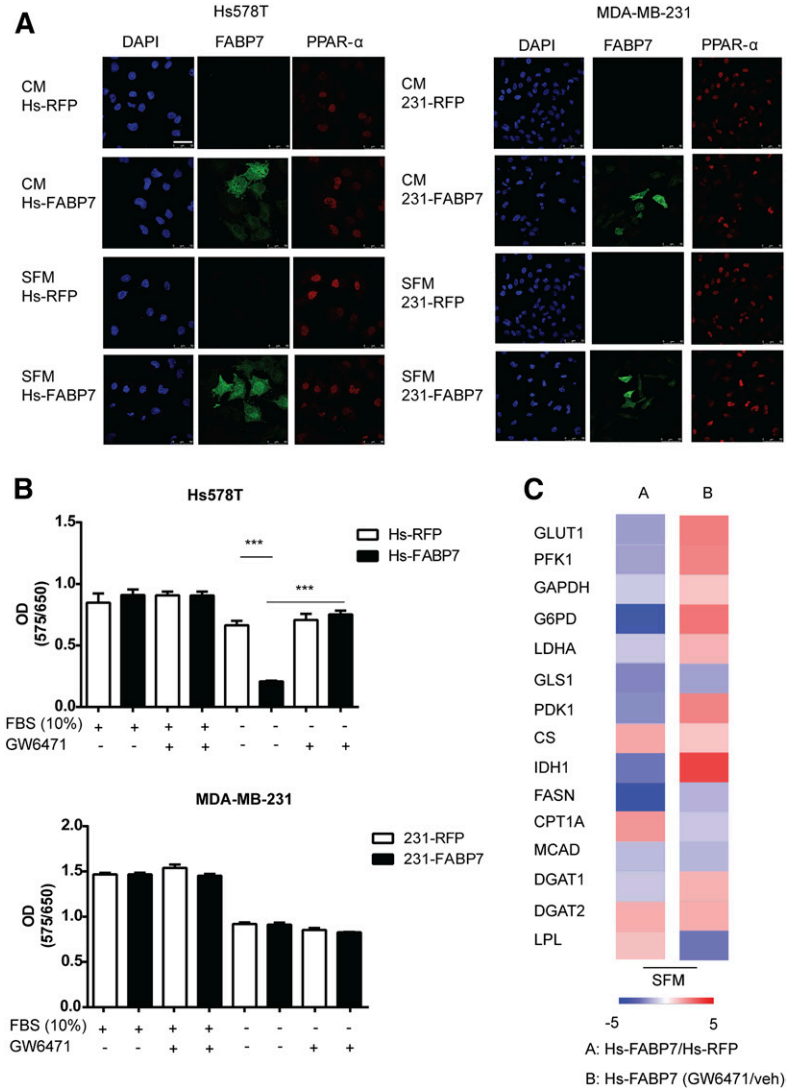

Fig. 5. FABP7-induced cell death in Hs578T cells during serum starvation was mediated by the action of PPAR-α signaling. A: Confocal microscopy of immunofluorescence staining of FABP7 (green) and PPAR-α (red) proteins in Hs578T and MDA-MB-231 cells after culture in either complete medium or serum-free medium for 24 h. Blue, DAPI. Scale bar, 50 μm. Data shown are representative of two independent experiments. B: Cells were treated with PPAR-α inhibitor GW6471 (2 μM) in complete or serum-starved medium for 72 h, before analyzing for cell viability using an MTT assay. Data shown are mean ± SEM of triplicates; this is a representative of three independent experiments. *** $P < 0.0001$. C: mRNA expression of key metabolic genes after treatment with 2 μM GW6471 in Hs-FABP7 cells for 24 h in serum starvation when compared with vehicle-treated cells. The genes were normalized to housekeeping gene 18S rRNA. CM, complete medium; SFM, serum-free medium.

role of FABP7 as a mediator for tumor cell death during nutrient-deprived conditions. This finding indicates an anti-tumorigenic role of FABP7 in TNBC, which is mediated by specific nutrient availability.

The metabolic vulnerabilities of FABP7-overexpressing Hs578T cells resulted in S/G2-phase arrest, which subsequently led to cell death. Serum starvation typically induces cell-cycle arrest at G1 phase (31, 32), which is observed in Hs-RFP and MDA-MB-231 cells. These cells were able to proliferate, despite a lower proliferation rate, indicating that the lower mitochondrial activity in these cells during serum starvation was sufficient to overcome the metabolic checkpoint and complete the cell cycle (33). Hs-FABP7 cells, however, arrested at the S/G2 phase. G2 arrest has been described as another growth-restricting mechanism in mitogen-starved conditions, likely due to elevated E2F activity (34). Cell arrest could potentially lead to cell death, in which both apoptosis and necrosis were observed in Hs-FABP7 cells upon serum starvation. Apoptosis is a cellular suicide program triggered by stress signals such as nutrient deprivation, which results in the execution of caspase-mediated cell death (35). Serum starvation has been shown to induce apoptosis in hepatocellular carcinoma cells (36) and MCF7 breast cancer cells (37), in which the latter was associated with an altered ratio of apoptosis regulating proteins Bax and Bcl-2. Necrosis, on the other hand, may occur when the minimal bioenergetic demands are not met (38), a condition similar to our observations where Hs-FABP7 cells may have limited bioenergetic substrates during serum starvation. In fact, there are common mediators of apoptosis and necrosis, which could potentially contribute to the two modes of cell death observed in our model (39). It is worth noting that FABP7 did not induce cell death in MDA-MB-231 cells during serum starvation, indicating that this cell line is probably more resilient to nutrient deprivation than Hs578T cells. The disparity in the response of Hs578T and MDA-MB-231 cells to serum starvation may also be attributed to differences in their metabolic profiles (40). Hence, it would be worthwhile to examine other TNBC cells with differing metabolic profiles, in delineating the molecular heterogeneity involved in cell death induced by metabolic vulnerabilities.

During serum starvation, cancer cells sense and adapt to nutrient deprivation by upregulating glucose metabolism

(41, 42), besides releasing fatty acids from the lipid droplet through lipolysis for β oxidation (24). Central to such adaption, PPAR-α is known to be a lipid sensor that maintains cellular energy homeostasis. It is a ligand-activated class of nuclear hormone receptor that binds to peroxisome proliferator response elements (PPREs) to induce transcription of genes such as lipid processing. Its activation aims at increasing lipid combustion in order to yield more energy production, especially in a challenged environment (43). It was shown in rat hepatocytes that PPAR-α expression is increased by fasting- and starvation-induced glucocorticoids (44), suggesting the role of PPAR-α to maintain cell survival.

In our model, increased PPAR-α expression was observed when the cells were serum-starved, possibly as an adaptation strategy of the cells. The activation of PPAR-α was observed in Hs-FABP7 cells during serum starvation, as reflected in the increase of PPAR-α target genes, CPT1A and MCAD, which are involved in fatty acid mitochondrial uptake and oxidation (45). Our observation may indicate the usage of fatty acids liberated from lipid droplets as the substrates for FAO. However, the attempt of the cells to survive serum starvation failed as the lipid storage was limited and fatty acids were absent in the serum-free media. In addition, PPAR-α activation also potentially inhibited glucose metabolism by targeting the consensus PPRE motif in the promoter region of Glut1, hence repressing its transcription (46). As a result, Hs-FABP7 cells could not efficiently utilize glucose as bioenergetic substrates when serum-starved, which eventually led to cell death.

Our data suggest that PPAR-α-induced changes are FABP7-dependent. Literature evidence shows that in Cos-7 cells where FABPs and PPAR-α are not detected, transfection of the proteins showed that PPAR-α activity is amplified by FABP1 and FABP2 (47). In another study, PPAR-α transactivation is proportional to levels of L-FABP in human hepatoma HepG2 cells line (48). In our model, upon serum starvation, increased nuclear FABP7 expression was observed, suggesting the role of FABP7 as fatty acids chaperones to transport PPAR-α ligands into the nucleus for PPAR-α activation. In murine L cells, transduction with FABP1 had dramatically enhanced the uptake of fatty acid into the nucleus (49). Incubation of rat liver nuclei with fluorescence-tagged FABP1 together with fatty acids demonstrated a strong fluorescence response in the nuclei, which otherwise did not happen when fatty acids were absent (50). There has been evidence indicating physical interaction between FABP1 and PPAR-α in primary hepatocytes (51). Ablation of L-FABP gene expression significantly impaired fatty acid distribution in the nucleus and affected PPAR-α activation in these cells (52). Hence, whether FABP7 and PPAR-α require direct contact to induce cell death in TNBC needs to be further investigated. In short, our data suggest that FABP7 facilitates PPAR-α activation in serum-starved condition by transporting its ligand (fatty acids) into the nucleus, before enhancing its transcriptional activity.

Our study provides an understanding on the role of FABP7 in regulating the metabolic adaptation of TNBC cell lines. Transcriptional activation of PPAR-α in FABP7-overexpressing cell can limit their metabolic plasticity when challenged with serum starvation and resulted in reduced survival of these cells. Hence, manipulating metabolic stress in cells expressing FABP7 protein may potentially be an effective targeted therapeutic strategy in FABP7-positive TNBC patients.

REFERENCES

1. Kanapathy Pillai, S. K., A. Tay, S. Nair, and C-O. Leong. 2012. Triple-negative breast cancer is associated with EGFR, CK5/6 and c-KIT expression in Malaysian women. *BMC Clin. Pathol.* **12:** 18.
2. Dent, R., M. Trudeau, K. I. Pritchard, W. M. Hanna, H. K. Kahn, C. A. Sawka, L. A. Lickley, E. Rawlinson, P. Sun, and S. A. Narod. 2007. Triple-negative breast cancer: clinical features and patterns of recurrence. *Clin. Cancer Res.* **13:** 4429–4434.
3. Rodler, E., L. Korde, and J. Gralow. 2010. Current treatment options in triple negative breast cancer. *Breast Dis.* **32:** 99–122.
4. Kaplan, H. G., and J. A. Malmgren. 2008. Impact of triple negative phenotype on breast cancer prognosis. *Breast J.* **14:** 456–463.
5. Zhang, Y., and J-M. Yang. 2013. Altered energy metabolism in cancer: a unique opportunity for therapeutic intervention. *Cancer Biol. Ther.* **14:** 81–89.
6. Obre, E., and R. Rossignol. 2015. Emerging concepts in bioenergetics and cancer research: metabolic flexibility, coupling, symbiosis, switch, oxidative tumors, metabolic remodeling, signaling and bioenergetic therapy. *Int. J. Biochem. Cell Biol.* **59:** 167–181.
7. Elstrom, R. L., D. E. Bauer, M. Buzzai, R. Karnauskas, M. H. Harris, D. R. Plas, H. Zhuang, R. M. Cinalli, A. Alavi, C. M. Rudin, et al. 2004. Akt stimulates aerobic glycolysis in cancer cells. *Cancer Res.* **64:** 3892–3899.
8. Wise, D. R., R. J. DeBerardinis, A. Mancuso, N. Sayed, X-Y. Zhang, H. K. Pfeiffer, I. Nissim, E. Daikhin, M. Yudkoff, S. B. McMahon, et al. 2008. Myc regulates a transcriptional program that stimulates mitochondrial glutaminolysis and leads to glutamine addiction. *Proc. Natl. Acad. Sci. USA.* **105:** 18782–18787.
9. Buzzai, M., D. E. Bauer, R. G. Jones, R. J. DeBerardinis, G. Hatzivassiliou, R. L. Elstrom, and C. B. Thompson. 2005. The glucose dependence of Akt-transformed cells can be reversed by pharmacologic activation of fatty acid β-oxidation. *Oncogene.* **24:** 4165–4173.
10. Olson, K. A., J. C. Schell, and J. Rutter. 2016. Pyruvate and metabolic flexibility: illuminating a path toward selective cancer therapies. *Trends Biochem. Sci.* **41:** 219–230.
11. Beloribi-Djefaflia, S., S. Vasseur, and F. Guillaumond. 2016. Lipid metabolic reprogramming in cancer cells. *Oncogenesis.* **5:** e189.
12. Baenke, F., B. Peck, H. Miess, and A. Schulze. 2013. Hooked on fat: the role of lipid synthesis in cancer metabolism and tumour development. *Dis. Model. Mech.* **6:** 1353–1363.
13. Zhao, J., Z. Zhi, C. Wang, H. Xing, G. Song, X. Yu, Y. Zhu, X. Wang, X. Zhang, and Y. Di. 2017. Exogenous lipids promote the growth of breast cancer cells via CD36. *Oncol. Rep.* **38:** 2105–2115.
14. Mashima, T., H. Seimiya, and T. Tsuruo. 2009. De novo fatty-acid synthesis and related pathways as molecular targets for cancer therapy. *Br. J. Cancer.* **100:** 1369–1372.
15. Tang, X. Y., S. Umemura, H. Tsukamoto, N. Kumaki, Y. Tokuda, and R. Y. Osamura. 2010. Overexpression of fatty acid binding protein-7 correlates with basal-like subtype of breast cancer. *Pathol. Res. Pract.* **206:** 98–101.
16. Shi, Y. E., J. Ni, G. Xiao, Y. E. Liu, A. Fuchs, G. Yu, J. Su, J. M. Cosgrove, L. Xing, M. Zhang, et al. 1997. Antitumor activity of the novel human breast cancer growth inhibitor, mammary-derived growth inhibitor-related gene, MRG. *Cancer Res.* **57:** 3084–3091.
17. Spitsberg, V. L., E. Matitashvili, and R. C. Gorewit. 1995. Association and coexpression of fatty-acid-binding protein and glycoprotein CD36 in the bovine mammary gland. *Eur. J. Biochem.* **230:** 872–878.
18. Burrier, R. E., C. R. Manson, and P. Brecher. 1987. Binding of acyl-CoA to liver fatty acid binding protein: effect on acyl-CoA synthesis. *Biochim. Biophys. Acta.* **919:** 221–230.
19. Coe, N. R., M. A. Simpson, and D. A. Bernlohr. 1999. Targeted disruption of the adipocyte lipid-binding protein (aP2 protein) gene

impairs fat cell lipolysis and increases cellular fatty acid levels. *J. Lipid Res.* **40:** 967–972.
20. Liu, R. Z., K. Graham, D. D. Glubrecht, R. Lai, J. R. Mackey, and R. Godbout. 2012. A fatty acid-binding protein 7/RXRβ pathway enhances survival and proliferation in triple-negative breast cancer. *J. Pathol.* **228:** 310–321.
21. Alshareeda, A. T., E. A. Rakha, C. C. Nolan, I. O. Ellis, and A. R. Green. 2012. Fatty acid binding protein 7 expression and its subcellular localization in breast cancer. *Breast Cancer Res. Treat.* **134:** 519–529.
22. Zhang, H., E. A. Rakha, G. Ball, I. Spiteri, M. Aleskandarany, E. Paish, D. G. Powe, R. D. Macmillan, C. Caldas, I. O. Ellis, et al. 2010. The proteins FABP7 and OATP2 are associated with the basal phenotype and patient outcome in human breast cancer. *Breast Cancer Res. Treat.* **121:** 41–51.
23. Mita, R., M. J. Beaulieu, C. Field, and R. Godbout. 2010. Brain Fatty Acid-binding Protein and ω-3/ω-6 fatty acids: mechanistic insight into malignant glioma cell migration. *J. Biol. Chem.* **285:** 37005–37015.
24. Rambold, A. S., S. Cohen, and J. Lippincott-Schwartz. 2015. Fatty acid trafficking in starved cells: regulation by lipid droplet lipolysis, autophagy, and mitochondrial fusion dynamics. *Dev. Cell.* **32:** 678–692.
25. Yang, Y., E. Spitzer, N. Kenney, W. Zschiesche, M. Li, A. Kromminga, T. Müller, F. Spener, A. Lezius, J. H. Veerkamp, et al. 1994. Members of the fatty acid binding protein family are differentiation factors for the mammary gland. *J. Cell Biol.* **127:** 1097–1109.
26. Kuhar, S. G., L. Feng, S. Vidan, M. E. Ross, M. E. Hatten, and N. Heintz. 1993. Changing patterns of gene expression define four stages of cerebellar granule neuron differentiation. *Development.* **117:** 97–104.
27. Arai, Y., N. Funatsu, K. Numayama-Tsuruta, T. Nomura, S. Nakamura, and N. Osumi. 2005. Role of Fabp7, a downstream gene of Pax6, in the maintenance of neuroepithelial cells during early embryonic development of the rat cortex. *J. Neurosci.* **25:** 9752–9761.
28. Kipp, M., T. Clarner, S. Gingele, F. Pott, S. Amor, P. van der Valk, and C. Beyer. 2011. Brain lipid binding protein (FABP7) as modulator of astrocyte function. *Physiol. Res.* **60 (Suppl. 1):** S49–S60.
29. Bensaad, K., E. Favaro, C. A. Lewis, B. Peck, S. Lord, J. M. Collins, K. E. Pinnick, S. Wigfield, F. M. Buffa, J. L. Li, et al. 2014. Fatty acid uptake and lipid storage induced by HIF-1α contribute to cell growth and survival after hypoxia-reoxygenation. *Cell Reports.* **9:** 349–365.
30. Lacroix, M. 2009. MDA-MB-435 cells are from melanoma, not from breast cancer. *Cancer Chemother. Pharmacol.* **63:** 567.
31. Shin, J-S., S-W. Hong, S-L. O. Lee, T-H. Kim, I-C. Park, S-K. An, W. K. Lee, J. S. Lim, K. I. Kim, Y. Yang, et al. 2008. Serum starvation induces G1 arrest through suppression of Skp2–CDK2 and CDK4 in SK-OV-3 cells. *Int. J. Oncol.* **32:** 435–439.
32. Huang, Y., Z. Fu, W. Dong, Z. Zhang, J. Mu, and J. Zhang. 2018. Serum starvation-induces down-regulation of Bcl-2/Bax confers apoptosis in tongue coating-related cells in vitro. *Mol. Med. Rep.* **17:** 5057–5064.
33. Schieke, S. M., J. P. McCoy, Jr., and T. Finkel. 2008. Coordination of mitochondrial bioenergetics with G1 phase cell cycle progression. *Cell Cycle.* **7:** 1782–1787.
34. Foijer, F., and H. te Riele. 2006. Restriction beyond the restriction point: mitogen requirement for G2 passage. *Cell Div.* **1:** 8.
35. Matsuura, K., K. Canfield, W. Feng, and M. Kurokawa. 2016. Metabolic regulation of apoptosis in cancer. *Int. Rev. Cell. Mol. Biol.* **327:** 43–87.
36. Kou, X., Y. Jing, W. Deng, K. Sun, Z. Han, F. Ye, G. Yu, Q. Fan, L. Gao, Q. Zhao, et al. 2013. Tumor necrosis factor-α attenuates starvation-induced apoptosis through upregulation of ferritin heavy chain in hepatocellular carcinoma cells. *BMC Cancer.* **13:** 438.
37. Tovar Sepulveda, V. A., X. Shen, and M. Falzon. 2002. Intracrine PTHrP protects against serum starvation-induced apoptosis and regulates the cell cycle in MCF-7 breast cancer cells. *Endocrinology.* **143:** 596–606.
38. Jin, S., R. S. DiPaola, R. Mathew, and E. White. 2007. Metabolic catastrophe as a means to cancer cell death. *J. Cell Sci.* **120:** 379–383.
39. Nikoletopoulou, V., M. Markaki, K. Palikaras, and N. Tavernarakis. 2013. Crosstalk between apoptosis, necrosis and autophagy. *Biochim. Biophys. Acta.* **1833:** 3448–3459.
40. Lanning, N. J., J. P. Castle, S. J. Singh, A. N. Leon, E. A. Tovar, A. Sanghera, J. P. MacKeigan, F. V. Filipp, and C. R. Graveel. 2017. Metabolic profiling of triple-negative breast cancer cells reveals metabolic vulnerabilities. *Cancer Metab.* **5:** 6.
41. Zheng, N., K. Wang, J. He, Y. Qiu, G. Xie, M. Su, W. Jia, and H. Li. 2016. Effects of ADMA on gene expression and metabolism in serum-starved LoVo cells. *Sci. Rep.* **6:** 25892.
42. Dai, S., A. Gocher, L. Euscher, and A. Edelman. 2016. Serum starvation induces a rapid increase of Akt phosphorylation in ovarian cancer cells. *FASEB J.* **30 (Suppl. 1):** 714.9.
43. Pyper, S. R., N. Viswakarma, S. Yu, and J. K. Reddy. 2010. PPARα: energy combustion, hypolipidemia, inflammation and cancer. *Nucl. Recept. Signal.* **8:** e002.
44. Viana Abranches, M., F. C. Esteves de Oliveira, and J. Bressan. 2011. Peroxisome proliferator-activated receptor: effects on nutritional homeostasis, obesity and diabetes mellitus. *Nutr. Hosp.* **26:** 271–279.
45. Mandard, S., M. Müller, and S. Kersten. 2004. Peroxisome proliferator-activated receptor α target genes. *Cell. Mol. Life Sci.* **61:** 393–416.
46. You, M., J. Jin, Q. Liu, Q. Xu, J. Shi, and Y. Hou. 2017. PPARα promotes cancer cell Glut1 transcription repression. *J. Cell. Biochem.* **118:** 1556–1562.
47. Hughes, M. L., B. Liu, M. L. Halls, K. M. Wagstaff, R. Patil, T. Velkov, D. A. Jans, N. W. Bunnett, M. J. Scanlon, and C. J. Porter. 2015. Fatty acid-binding proteins 1 and 2 differentially modulate the activation of peroxisome proliferator-activated receptor α in a ligand-selective manner. *J. Biol. Chem.* 290: 13895–13906.
48. Wolfrum, C., C. M. Borrmann, T. Börchers, and F. Spener. 2001. Fatty acids and hypolipidemic drugs regulate peroxisome proliferator-activated receptors α-and γ-mediated gene expression via liver fatty acid binding protein: a signaling path to the nucleus. *Proc. Natl. Acad. Sci. USA.* **98:** 2323–2328.
49. Huang, H., O. Starodub, A. McIntosh, A. B. Kier, and F. Schroeder. 2002. Liver fatty acid-binding protein targets fatty acids to the nucleus. Real time confocal and multiphoton fluorescence imaging in living cells. *J. Biol. Chem.* **277:** 29139–29151.
50. Lawrence, J. W., D. J. Kroll, and P. I. Eacho. 2000. Ligand-dependent interaction of hepatic fatty acid-binding protein with the nucleus. *J. Lipid Res.* **41:** 1390–1401.
51. Hostetler, H. A., A. L. McIntosh, B. P. Atshaves, S. M. Storey, H. R. Payne, A. B. Kier, and F. Schroeder. 2009. L-FABP directly interacts with PPARα in cultured primary hepatocytes. *J. Lipid Res.* **50:** 1663–1675.
52. McIntosh, A. L., B. P. Atshaves, H. A. Hostetler, H. Huang, J. Davis, O. I. Lyuksyutova, D. Landrock, A. B. Kier, and F. Schroeder. 2009. Liver type fatty acid binding protein (L-FABP) gene ablation reduces nuclear ligand distribution and peroxisome proliferator-activated receptor-α activity in cultured primary hepatocytes. *Arch. Biochem. Biophys.* **485:** 160–173.